ISBN: 978-3-95450-261-5 ISSN: 2673-7000 doi: 10.18429/JACoW-NAPAC2025-THP025

DEVELOPMENT OF SODIUM POTASSIUM ANTIMONIDE PHOTOCATHODES FOR USE OF COHERENT ELECTRON COOLING*

K. P. Mondal[1,†], R. Begay[1], L. Cultrera[1], M. Gaowei[1], J. Walsh[1], Y. Yang [2]
[1]Brookhaven National Laboratory, Upton, NY, USA
[2]State University of New York at Stony Brook, Stony Brook, NY, USA

Abstract

Alkali antimonide photocathodes are promising candidates for high-brightness electron sources due to their high quantum efficiency (QE), fast response time, and compatibility with ultra-high vacuum systems. In this work, we report the growth and characterization of Na-K-Sb photocathodes using a custom-built UHV deposition system developed for Coherent Electron Cooling (CeC) applications. Photocathodes were fabricated via sequential deposition of Sb, K, and Na on Mo substrates, followed by optimization of deposition parameters to maximize QE and ensure spatial uniformity. QE maps revealed uniform photocathode response with values reaching ~3.5%, while additional Sb-K "yo-yo" layers further enhanced QE to ~7% with moderate trade-off in uniformity. The films exhibit good thermal and vacuum stability, highlighting their suitability for long-duration accelerator operations. These results demonstrate both the reproducibility and performance potential of Na-K-Sb photocathodes for advanced photoinjector systems.

INTRODUCTION

The Coherent Electron Cooling (CeC) scheme marks a significant advancement in accelerator technology by enabling rapid phase-space cooling of ion beams [1-4]. This method is especially vital for future high-luminosity facilities such as the Electron-Ion Collider (EIC), where maintaining high beam brightness and low emittance is essential for achieving design performance targets [5].

CeC is the photoinjector, which relies on robust photocathodes capable of generating high-current, low-emittance electron beams with minimal dark current and long operational lifetimes. Alkali antimonide photocathodes have emerged as strong candidates due to their combination of high quantum efficiency (QE), fast temporal response, and improved stability in vacuum [6-7].

In particular, Na-K-Sb photocathodes offer better thermal and vacuum stability than more conventional alkali antimonide variants like Cs_3Sb and K_2CsSb. These qualities make them especially attractive for long-duration accelerator operations [8-9].

Beyond QE, the spatial uniformity of the photocathode's QE plays a critical role in determining beam quality. Non-uniform QE distribution can lead to the increase of mean transverse emittance (MTE), current density modulation, and overall degradation of beam performance. Thus, optimizing both QE and its uniformity is crucial for high-brightness beam sources [10-11].

In this work, we report on the growth and characterization of Na-K-Sb photocathodes using a custom UHV photocathode growth system. We emphasize spatial QE uniformity, demonstrate reproducibility across multiple samples, and investigate techniques—such as Sb-K "yo-yo" method—to enhance QE without compromising stability or uniformity.

EXPERIMENTAL

Photocathodes were grown on polished molybdenum (Mo) pucks, which serve as stable and inert substrates for alkali antimonide films. Prior to deposition, the pucks were annealed at 400 °C for 7 hours under ultra-high vacuum (base pressure ~10^{-11} Torr) to remove surface contaminants and improve film adhesion.

Na-K-Sb photocathodes were synthesized using sequential deposition of antimony (Sb), potassium (K), and sodium (Na) in a UHV system (Fig. 1) equipped with in-situ QE monitoring and post-growth QE mapping capabilities. Sb was deposited using a thermal evaporator at a thickness of ~15 nm and a rate of ~2 nm/min under a base pressure of 1.5×10^{-11} Torr. Potassium and sodium were deposited using SAES getter sources, with typical K deposition rates of ~0.8 nm/min.

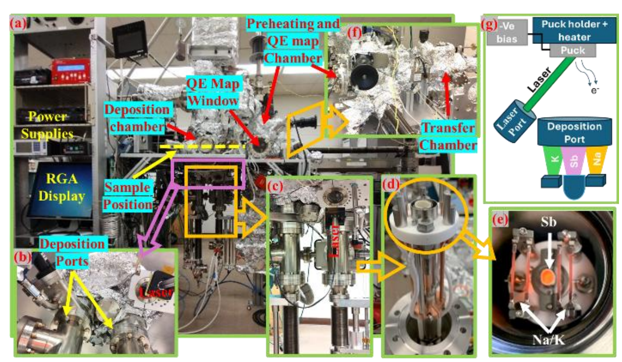

Figure 1: (a) The BNL UHV CeC photocathode growth system at IO, BNL, with in situ QE and QE map measurements, (c) magnified view of attached tube having source cluster inside, (d) both source clusters with electrical connection and crucible, (e) top view of source cluster having alkali material getter source and Sb crucible are indicated, (f) magnified perpendicular view the system where transfer chamber is indicated, (g) schematic of sequential/co-evaporation [12].

The film thickness and deposition rates were monitored using a quartz crystal microbalance (QCM). The substrate temperature was maintained at 90 °C during Sb deposition

* Work is supported by Brookhaven Science Associates, LLC under Contract No. DE-SC0012704 with the U.S. Department of Energy
† kmondal@bnl.gov

ISBN: 978-3-95450-261-5 ISSN: 2673-7000 doi: 10.18429/JACoW-NAPAC2025-THP025

and increased to 135 °C during K and Na deposition. QE was monitored in real-time, and deposition parameters were optimized to follow the QE growth curve and maximize overall photocathode performance.

To further enhance QE, an Sb-K “yo-yo” deposition technique was employed on top of the standard Na-K-Sb layer, resulting in the final structure: K–Sb(yo-yo)/Na–K–Sb/Mo.

Spatially resolved QE maps were obtained post-growth to assess uniformity and reproducibility.

RESULTS AND DISCUSSION

Multiple Na-K-Sb photocathodes were developed with the goal of achieving high QE and excellent spatial uniformity. One representative photocathode used in CeC testing is shown in Fig. 2. Figure 2(a) displays the QE evolution during sequential deposition of Sb, K, and Na. K step was stopped at % QE. QE started increasing upon Na deposition and eventually reaching ~2.4%.

The corresponding 2D QE map in Fig. 2(b) reveals a mostly uniform QE distribution with only minor edge variations, likely due to flux gradients caused by mask. A 3D representation of the QE surface (Fig. 2(c)) further confirms the near-uniformity and validates the stability of the growth process.

To demonstrate improvements in uniformity, Fig. 3(a) compares a photocathode grown in earlier trials. Process optimizations—including more uniform flux distribution, better temperature control, and deposition rate tuning—resulted in visibly enhanced uniformity in later samples. Fig. 3(b) shows a 3D QE map of another photocathode that achieved QE of ~3.5% with uniform distribution, highlighting reproducibility and process consistency.

To further boost QE, an Sb-K “yo-yo” deposition was performed on a Na-K-Sb base. This approach yielded a QE of approximately 7%, as shown in Fig. 3(c). However, this enhanced QE came with a slight trade-off in spatial uniformity, mainly near edge. The QE map of the yo-yo-coated sample revealed some localized variations, suggesting that while QE was significantly improved, further optimization is required to achieve both high QE and excellent uniformity simultaneously.

In addition, preliminary thermal stability tests on Na-K-Sb photocathodes indicate better resistance to decomposition than traditional alkali antimonides, supporting their suitability for long-duration accelerator operations. These results will be presented in a separate study.

CONCLUSION AND FUTURE PLANS

We have successfully developed Na-K-Sb photocathodes with QE up to ~3.5% with good spatial uniformity, suitable for high-brightness applications such as Coherent Electron Cooling (CeC). Further enhancement to ~7% QE was achieved via additional Sb-K “yo-yo” deposition, although at the cost of reduced uniformity at one edge.

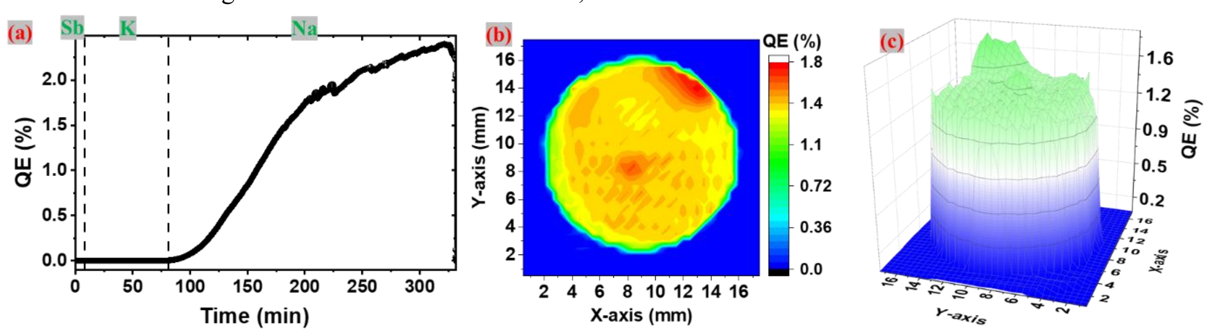

Figure 2: (a) QE evolution during sequential deposition of Sb, K, and Na for Na-K-Sb photocathode growth, (b) 2D spatial map showing the QE distribution across the photocathode surface, and (c) 3D representation of the QE distribution with QE plotted along the z-axis.

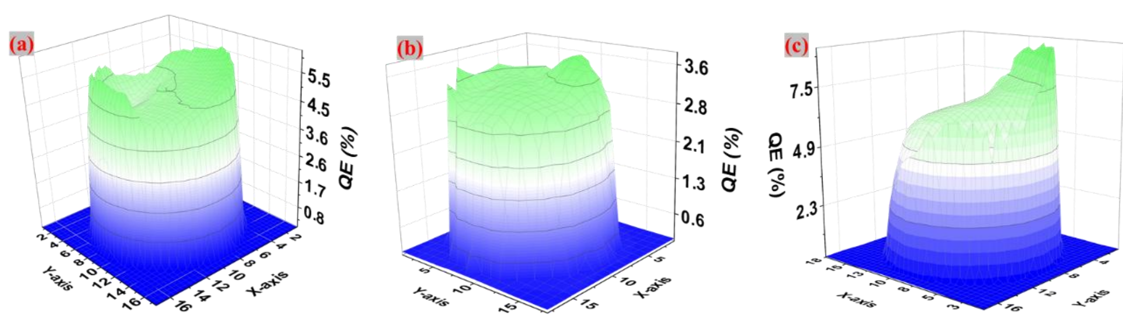

Figure 3: 3D quantum efficiency (QE) maps of Na-K-Sb photocathodes: (a) Early-stage photocathode showing non-uniform QE distribution, (b) Optimized growth yielding uniform QE with decent efficiency, (c) Final photocathode structure with additional Sb–K "yo-yo" layer, achieving higher QE (~7%) with moderate uniformity.

ISBN: 978-3-95450-261-5 ISSN: 2673-7000 doi: 10.18429/JACoW-NAPAC2025-THP025

These results demonstrate the reproducibility and performance potential of Na-K-Sb photocathodes grown using the CeC deposition system. Their improved thermal stability compared to Cs- and K-based antimonides makes them strong candidates for next-generation photoinjectors.

Future work will focus on: Further refining the yo-yo process to maintain both high QE and spatial uniformity.

Investigating co-deposition approaches to directly grow stoichiometric Na_2KSb photocathodes.

Conducting comprehensive thermal stress testing and long-term operational lifetime studies.

REFERENCES

[1] V. N. Litvinenko and Y. S. Derbenev, "Coherent electron cooling," *Phys. Rev. Lett.*, vol. 102, no. 11, p. 114801, Mar. 2009. doi:10.1103/physrevlett.102.114801

[2] J. Ma, G. Wang, and V. Litvinenko, "Simulations of coherent electron cooling with two types of amplifiers," *Int. J. Mod. Phys. A*, vol. 34, no. 36, p. 1942029, Dec. 2019. doi:10.1142/s0217751x19420296

[3] Y. S. Derbenev and V. Litvinenko, "FELs and high-energy electron cooling," in *Proc. FEL'07*, Novosibirsk, Russia, Aug. 2007, paper TUCAU01, pp. 268-275.

[4] V. Litvinenko, "Coherent electron cooling," in *Proc. PAC'09*, Vancouver, Canada, May 2009, paper FR1GRI01, pp. 4236-4240.

[5] E. Wang *et al.*, "The accelerator design progress for EIC strong hadron cooling," in *Proc. IPAC'21*, Campinas, Brazil, May 2021, pp. 1424-1427. doi:10.18429/JACoW-IPAC2021-TUPAB036

[6] M. Gaowei *et al.*, "Codeposition of ultrasmooth and high quantum efficiency cesium telluride photocathodes," *Phys. Rev. Accel. Beams*, vol. 22, no. 7, Jul. 2019. doi:10.1103/physrevaccelbeams.22.073401

[7] Z. Ding *et al.*, "*In-situ* synchrotron x-ray characterization of K2CsSb photocathode grown by ternary co-evaporation," *J. Appl. Phys.*, vol. 121, no. 5, p. 055305, Feb. 2017. doi:10.1063/1.4975113

[8] L. Cultrera *et al.*, "Growth and characterization of rugged sodium potassium antimonide photocathodes for high brilliance photoinjector," *Appl. Phys. Lett.*, vol. 103, no. 10, p. 103504, Sep. 2013. doi:10.1063/1.4820132

[9] C. Xu, R. Schier, and C. Cocchi, "Electronic and optical properties of computationally predicted Na–K–Sb crystals," *Electron. Struct.*, vol. 7, no. 1, p. 015001, Jan. 2025. doi:10.1088/2516-1075/adaab8

[10] D. H. Dowell and J. F. Schmerge, "Quantum efficiency and thermal emittance of metal photocathodes," *Phys. Rev. Spec. Top. Accel Beams*, vol. 12, no. 7, p. 074201, Jul. 2009. doi:10.1103/physrevstab.12.074201

[11] David H. Dowell, "Sources of emittance in rf photocathode injectors: intrinsic emittance, space charge forces due to non-uniformities, RF and solenoid effects," Nov. 2016, arXiv:1610.01242. doi:10.48550/arXiv.1610.01242

[12] K. P. Mondal, R. Begay, J. Biswas, L. Cultrera, M. Gaowei, and J. Walsh, "An upgrade for the CeC cathode deposition system: co-deposition of K_2CsSb and CsTe/GaAs for CeC use," in *Proc. IPAC'24*, Nashville, TN, USA, May 2024, pp. 2060-2063. doi:10.18429/JACoW-IPAC2024-WEPC43